Cancer Management and Research

Dovepress

open access to scientific and medical research

Open Access Full Text Article

ORIGINAL RESEARCH

Investigating the Metabolic Level of Endogenous and Exogenous Substances on the Intervention of Traditional Chinese Medicine Fuzheng Yiliu Decoction in a Rat Orthotopic Liver Cancer Model

Hongcheng Zhang[1,2,*], Qiwen Dai[1,2,*], Maogui Zeng[1], Yingying Liu[1], Jian Du[2], Wensheng Pang[2], Juan Hu[1,2], Liwu Chen[1]

[1]The Second Affiliated Hospital of Fujian University of Traditional Chinese Medicine, Fuzhou, 350003, People's Republic of China; [2]The School of Pharmacy, Fujian University of Traditional Chinese Medicine, Fuzhou, 350122, People's Republic of China

*These authors contributed equally to this work

Correspondence: Juan Hu; Liwu Chen, The Second Affiliated Hospital Fujian University of Traditional Chinese Medicine, Fuzhou, 350003, People's Republic of China, Email huj@fjtcm.edu.cn; chenlw_2022@163.com

Background: Fuzheng Yiliu decoction (FZYLD), a Chinese formula consisting of four herbs, can be clinically used as an adjuvant therapy after surgery or palliative treatment for advanced liver cancer.

Methods: This study identified the endogenous and exogenous metabolites of FZYLD in rat serum to characterize the underlying mechanism of its antitumor activity, as well as relieving cancer-related weakness. An orthotopic transplantation rat model of HepG2 cells was established and administered with FZYLD by gastric perfusion for 14 days. Cardiopulmonary function and tail suspension test were used to evaluate the bodily weakness of hepatocellular carcinoma (HCC) rats. Tumor weight and size were measured to calculate inhibition ratios. Serum of different concentrations of FZYLD was used to culture the 2-[N-(7-nitrobenz-2-oxa-1, 3-diaxol-4-yl) amino]-2-deoxyglucose-labeled HepG2 cells. IC_{50} value was measured using MTT assay. Endogenous and exogenous metabolites in rat serum were detected using nuclear magnetic resonance or LC-MS/MS spectroscopy.

Results: FZYLD improved cardiopulmonary function, decreased immobility time in tail suspension test, and yielded tumor inhibition ratios of up to 27%. Serum endogenous markers, such as lipoproteins (high- and low-density lipoproteins), glucose, and valine, and lactic acid metabolic disturbance were recovered, to some extent, in HCC rats. Exogenous metabolites, diosgenin, apigenin-7-O-acetyl-β-D-glucoside, calycosin-7-glucoside, calycosin, ganoderic-acid-A, formononetin, and methylnissolin, became detectable in the blood. FZYLD-containing serum substantially inhibited the proliferation of HepG2-cells. IC_{50} value was found to be 24.31%. Further, we confirmed that FZYLD could revert energy and lipid metabolism disorders and that its constituents could be bioactive components that induce apoptosis in cancer cells.

Conclusion: The present study explained the mechanism of the effect of FZYLD on body empty, fatigue, and low immunity in patients with cancer, offering an efficient way for research of natural compounds in traditional Chinese medicine.

Keywords: HCC rat model, Fuzheng Yiliu decoction, regulation of metabolic balance, ameliorating cancer-related weakness, anti-liver tumor

Introduction

Traditional Chinese medicine dates back more than 2000 years ago. As the first line of defense in maintaining health and combating disease, traditional Chinese medicine plays an important role in the Chinese health care system. The Chinese pharmacopeia contains thousands of substances of plant, animal, or mineral origin, most of which are herbs.[1–6]

Fuzheng Yiliu decoction (FZYLD), a multi-herb formula that consists of four herbs: *Radix astragali, Fructus ligustri lucidi, Ganoderma*, and *Rhizoma dioscoreae*, has been clinically employed, more than 10 years ago, for the management

Received: 29 June 2022
Accepted: 1 September 2022
Published: 17 September 2022

Graphical Abstract

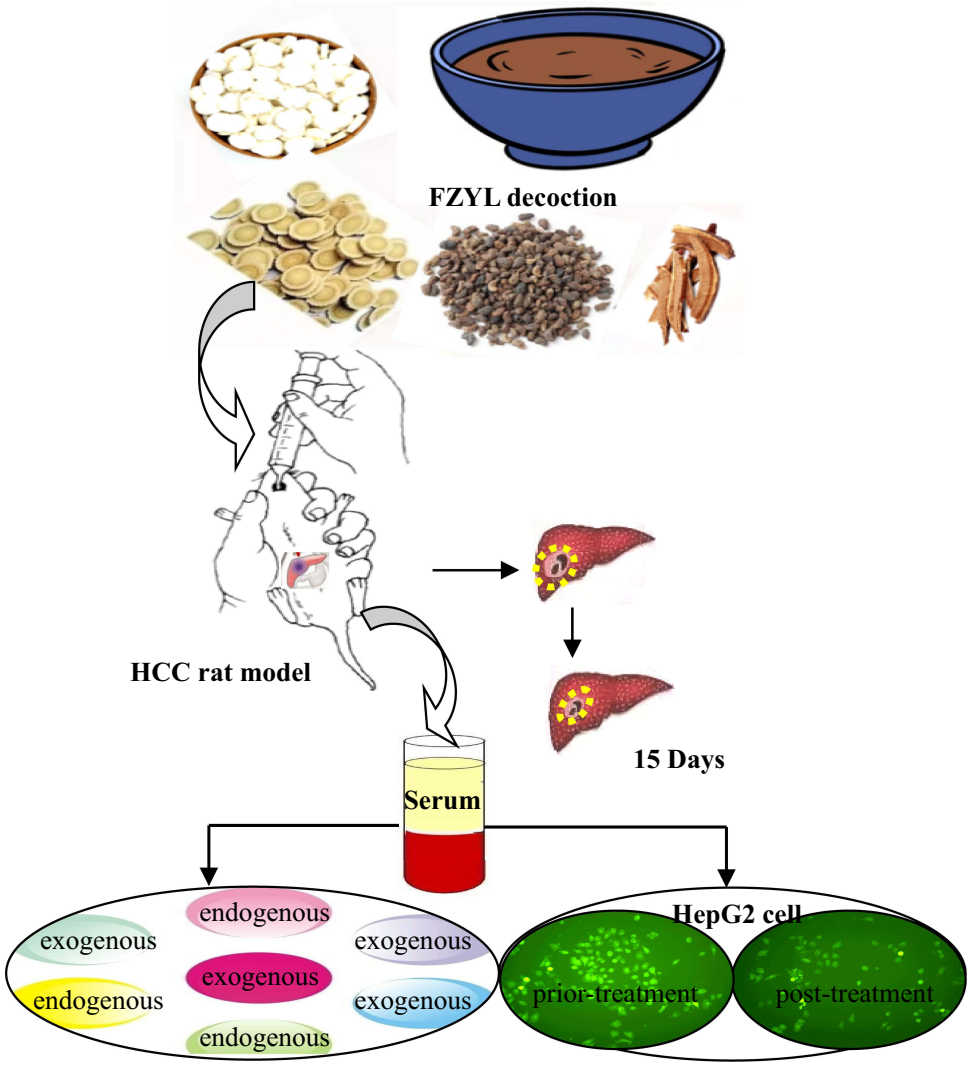

of alimentary canal neoplasms. Moreover, it can improve the clinical symptoms, delay body weakening, and prolong the survival time of patients with tumors.[7–9] Further, FZYLD was found to upregulate the expression of apoptosis-related markers, Bax and p53, in H22 tumor-bearing mice and substantially decrease the expression of a proliferation-inducing ligand in ICR mice,[10–12] showing that FZYLD may have multiple targets in the management of anticancer metastasis process.[13]

Our previous studies identified 21 chief constituents in FZYLD chemical composition: daidzin, ganoderiol F, specnuezhenide, calycosin-7-O-β-D-glucoside, calycosin, apigenin-7-glucoside, luteolin-7-O-β-D-glucoside, luteolin, ononin, oleanolic acid-3-acetate, ganode-8-en-ric acid A, ganoderic acid D, ganoderic acid G, ganoderic acid B, formononetin, ganoderic acid C2, ganoderic acid A, ganoderic acid H, ganoderic acid F, astragaloside IV, and diosgenin-3-di-b-O-glucopyranoside. The contents of the four flavonoids, calycosin-7-O-β-D-glucoside, ononin, calycosin, and formononetin, in *Radix astragali* were determined to be 0.38, 0.30, 0.18, and 0.53 mg/g, respectively. Additionally, the contents of ganoderic acids, ganoderic acid G, ganoderic acid B, ganoderic acid C2, ganoderic acid A, and ganoderic acid H, in *Ganoderma* were 0.32, 0.29, 0.17, 0.24, and 0.27 mg/g, respectively. Moreover, the contents of astragaloside IV, specnuezhenide, and diosgenin were 0.22, 0.19, and 0.19 mg/g, respectively.[14]

Molecular docking studies for B-cell lymphoma extra-large (Bcl-XL), interleukin (IL)-2, and tumor necrosis factor-α (TNF-α) were used to evaluate the anticancer activity of FZYLD. HepG2 cells were used for in vitro evaluation of the killing effect of FZYLD-activated natural killer (NK) cells that regulate the immune response by modulating IL-2 and TNF-α expression. In the "Fuzheng" Chinese medicine formula, many substances participate in the complex regulation of the immune network to execute the anti-tumor effects.[14,15]

Metabonomics, which covers an impressive and ever-increasing amount of endogenous compounds, focuses on the holistic investigation of multi-parametric metabolite responses of living systems, consistent with the overall concept and theory of traditional Chinese medicine.[16] Nuclear magnetic resonance (NMR) spectroscopic analysis coupled with principal component analysis (PCA) and orthogonal signal correction-partial least squares (OSC-PLS) methods offers a powerful new approach for the assessment of metabolic function. Moreover, Carr-Purcell-Meiboom-Gill (CPMG) and Longitudinal eddy-delay (LED) have been used for pattern recognition.[17]

Many active ingredients are present in the traditional Chinese Medicine formula. High-performance liquid chromatography (HPLC)-mass spectroscopy (MS) is among the analytical techniques that can be used for phytochemical research and has been widely applied to investigate the substance basis of the pharmacodynamics of traditional Chinese medicine.[18–20]

HepG2, an immortalized cell line that consists of human liver carcinoma cells, is commonly used in drug metabolism and hepatotoxicity studies. HepG2 cells are inoculated in rats to create the HepG2 cell line-derived xenograft liver cancer model. The HepG2 xenograft of human hepatocellular carcinoma (HCC) is usually used to study the inhibitory effect on tumor growth.[21]

In this study, we established an orthotopic transplantation rat model of HepG2 cells and administered it with FZYLD by gastric perfusion for 14 days. Cardiopulmonary function and tail suspension test were used to examine the bodily weakness of HCC rats. Tumor weight and size were measured to calculate tumor inhibition ratios. Endogenous metabolites were assessed in HCC rat serum using NMR to investigate the potential biomarkers associated with the efficacy of FZYLD. Exogenous metabolites were identified using HPLC/MS to study the bioactive components of FZYLD in rat serum. Using serum pharmacologic method, 2-[N-(7-nitrobenz-2-oxa-1, 3-diaxol-4-yl) amino]-2-deoxyglucose (2-NBDG) was used to mark the HepG2 liver cancer cells. The change in cellular proliferation was observed at different time points with the aid of fluorescent microscopy, by co-culturing with different concentrations of serum-containing FZYLD. Further, we explored the mechanisms underlying the effect of Fuzheng Yiliu in improving body weight and fatigue in patients with tumor.

Materials and Methods

Herbal Materials and Chemicals

Radix astragali and *Ganoderma* made in Fuzhou Huichun Chinese medicine Yinpian Factory Co. Ltd. (batch number: 10010818 and 10010605), *Fructus ligustri lucid* made in Shanghai Leiyunshang Chinese medicine Yinpian Factory (batch number: 20110101), and *Rhizoma dioscoreae* made in Anhui Wansheng Chinese medicine Yinpian Factory Co. Ltd. (batch number: 110108).

Standard compounds were purchased from BioBioPha Co., Ltd., Kunming Institute of Botany and China, and China Shanghai Tauto Biotech Co., Ltd., with a purity up to 98% by HPLC. HPLC-grade acetonitrile was purchased from Thermo Fisher Scientific, (USA). D2O was purchased from Cambridge Isotope Laboratories, Inc., (USA), and 3-trimethylsilane-2,2,3,3-tetradeuterated sodium propionate (TSP) was procured from Merck & Co., Inc., (Germany). Other chemicals, including glacial acetic acid, were of analytical grade and purchased from commercial sources.

Instruments

A MedLab_Model U/4c501H bio-signal acquisition and processing system (MedLab) with a Model YP200 pressure transducer and Model HX200 pneumotachograph transducer (Nanjing Medease Science and Technology Co., Ltd., Nanjing, China), was employed.

A Waters Technologies Alliance 2695 separation module was equipped with an auto-sampler and a Waters 2996 photodiode array detector. Mass spectrometry was performed using a Quattro Micro mass spectrometer equipped with ESI and APCI probes and a tandem quadrupole analyzer. Control of the LC-MS/MS system and data acquisition were performed using a Masslynx 4.0 workstation (Milford, CT, USA). The INOVA 600 MHz high-resolution NMR spectrometer with pulsed field gradients was produced by Varian, Inc. equipped with the triple resonance (1H, 13C, 15N) Inverse 5 mm 13C Enhanced HCN Cold Probe (Lake Forest, California, USA).

Eppendorf MiniSpin Plus personal microcentrifuge was produced by Eppendorf AG (Hamburg, Germany). A TGL-16G high-speed refrigeration centrifuge and TDL-40B low speed centrifuge from Shanghai Anting Science Instrument Factory (Shanghai, China) and an SK-1fast mixer from Changzhou Guohua Electric Appliance Co., Ltd. (Changzhou, China) were also employed. Ultrapure water was prepared using a Milli-Q system (Millipore, MA, USA).

FZYLD Preparation

The four-herb mixture in the prescribed proportions was crushed to powder (60 smash). The total weight of a mixed 450.0-g dose included 150 g *Radix astragali*, 150 g *Ganoderma*, 75 g *Fructus ligustri lucid*, and 75 g *Rhizoma dioscoreae*. They were soaked in six times their weight of cold water for 30 min and let simmer for 20 min. A total of 1500 mL of the decoction was drained. Then, the process was repeated. Two filtrates were combined, filtrated again, and concentrated to 1 mL containing 0.45 g crude medicine.

In situ Liver Cancer Model in SD Rats Induced by HepG2 Cells

Specific-pathogen free, Sprague-Dawley (SD) male *adult* rats (250 ± 20 g) were obtained from Shanghai SLAC Laboratory Animal Co., Ltd. (Shanghai, China). Rats were allowed free access to tap water and were provided with standard rodent diet. The animals were maintained at 60% relative humidity and a 12 h light/dark cycle at ambient temperature. Rats were fasted for 12 h before the experiment. Animal experiments were carried out in accordance with the Guidelines for Institutional Animal Ethics and were approved by the Committee of the Second Affiliated Hospital of Fujian University of Traditional Chinese Medicine (License number: FJTCM-IAEC2011001).

HepG2 tumor cells were cultured in Dulbecco's Modified Eagle Medium (DMEM) supplemented with 10% fetal bovine serum (FBS). The liver cancer model was prepared by direct injection of HepG2 tumor cells into the rats. Rats were anesthetized using isoflurane, and 2×10^6 HepG2 cells were injected into the liver lobe to prepare the orthotopic transplantation model of human HCC.

Animal Experiment Protocol

Twenty-one SD rats were randomly divided into three groups (n = 7): model and low- and high-dose groups. Starting from the third day after surgery, FZYLD was administered to animals via gastric infusion. Based on clinical experience, the low-dose group received FZYLD at a dosage of 2.0 g/kg (equivalent clinically used dose), whereas the high dose group received FZYLD at a dosage of 4.0 g/kg (twice as much as the clinically used dose), twice a day, for a total of two weeks. The model group was administered an equal volume of saline.

Assessment of the Cardiopulmonary Function

After treatment, to observe the effect of FZYLD on cardiopulmonary function, rats were sedated using an intraperitoneal injection of 4 mL/kg of 10% chloral hydrate. Common carotid artery intubation, pressure transducer, and flow transducer were individually connected to the MedLab U/4c 501H biological signal acquisition and processing system. Fourteen days after FZYLD administration in HCC rats, parameters of cardiopulmonary function, including systolic blood pressure (SBP), diastolic blood pressure (DBP), heart rate (HR), tidal volume (Vt), airway flow (V), and transpulmonary pressure (Ptp), were recorded.

Tail Suspension Test

Tail suspension test was used to evaluate fatigue in rats. The tail of each rat was placed on a horizontal plate 1 m above the ground, with its sight blocked using a board on both sides. Initially, rats struggled to overcome the abnormal posture,

but after a certain period of time, intermittent immobility was observed. During a six-minute test period, the longer their immobility time, the greater their weakness.

Assessment of the tumor growth inhibition rate

Laparotomy was performed after FZYLD administration for 48 h. The tumor weight and size were measured. HCC model and treatment groups contrast analysis was used to calculate the tumor inhibition rate.

NMR Analysis of Endogenous Metabolites

At the end of the experiment, all rats were anesthetized, and blood samples were acquired via the abdominal aorta. The blood was centrifuged at 4 °C and 3000 rpm for 15 min. Supernatants (sera) were stored at 80 °C for NMR analysis. A total of 100 μL of TSP heavy water solution (1 mg/mL), 200 μL heavy water (D_2O), and 300 μL serum were added to the centrifuge tube. After shaking and mixing, the serum solution was centrifuged at 13,000 rpm for 10 min. The supernatant was added to 5-mm NMR tube.

Data were collected by relaxation editing pulse sequence (CPMG pulse sequence): -RD-90°- (t-180°-t) n-ACQ; and diffusion edit pulse sequence (LED bpp pulse sequence): -RD-90°-G1-180°-G1-90°-T-90°-G1-180°-G1-90°-t-90°-ACQ. Small molecule metabolites and lipid metabolites were observed in the serum. The spectrum width of the CPMG experiment was 8000 Hz, and the sampling number was 32 k. The sampling time was 2 s, the cumulative number was 64 times, τ 400 s, the relaxation delay was 2 s; a low power pulse was used to pressurize the water peak. The left peak of the lactic acid methyl signal was chosen as δ 1.33. The free inductive attenuated (free induction decay, FID) signal data were zeroed, and the line broadening factors of 0.5 Hz (CPMG experiment) and 3 Hz (LED bpp experiment) were added, and the 1H NMR spectrum was obtained by Fourier transform.

Chromatographic and Mass Spectrometric Analysis of Exogenous Metabolites

The blood was centrifuged at 4 °C and 3000 rpm for 15 min, and the serum was stored at −80 °C. Serum (1 mL)-containing drug was placed in a polystyrene tube. Then, eight times its volume of ethyl acetate-methanol (1:1) was added and vortexed for 5 min. This was followed by centrifugation for 10 min at 3500 rpm. The resulting supernatant liquid was dried by N_2 at 40 °C. Then, water (100 μL) and methanol (100 μL) were added, vortexed for 5 min, and centrifuged for 10 min at 12,000 rpm. The resulting supernatant liquid was analyzed by HPLC (20 μL injection volume) after filtration (0.22 μm micro-porous filtering film).

LC-MS/MS determination was achieved using a Waters XTerra®MS C18 (2.1 mm × 150 mm, 5 μm) column. The mobile phase was composed of acetonitrile (20 mmol/L)-ammonium acetate aqueous solution. The flow rate was set at 0.2 mL/min at 40.7 bar. The sample injection volume was 10 μL, and the detection wavelength was 260 nm. The gradient program included four steps: first, the ratio of acetonitrile was increased from 2 to 10% within 20 min, 10 to 45% within the next 20 min, and 45 to 70% within the following 10 min, until final acetonitrile concentration was 70% for the next 5 min.

Positive and negative ESIs were compared, and the response of positive ESI was found to be remarkably higher than that of negative ESI. Different cone-hole voltage (10–100 V), capillary voltage, and collision energy were investigated, and sensitivity for the fragment ions was compared to optimize the mass spectral conditions (Table 1).

Table 1 Parameters of Mass Spectrometric Analysis

Parameters	Setting Value	Parameters	Setting Value
Ion source	ESI	Detection mode	Positive/negative ion
Detection range (m/z)	200–800	Capillary voltage	3KV(+)/2.5KV(-)
Cone-hole voltage	30V	Two-stage cone-hole voltage	3V
Desolvent gas temperature	300°C	Ion source temperature	120°C
Desolvation gas flow rate	350 L·hr^{-1}	Cone-hole gas flow	50 L·hr^{-1}

Determination of the Effect of FZYLD-Containing Serum on HepG2 Cell Proliferation

SD rats were randomly divided into model control and test groups. The test group was perfused with FZYLD at a dose of 2.0 g/kg (equivalent clinical dose), whereas the model control group was perfused with an equal volume of saline for 10 days. After fasting for 12 h and 40 min after the last administration, rats were anesthetized using ethyl carbamate injection (1.5 g/kg body weight), and blood samples (3 mL) were acquired via the abdominal aorta. Blood was centrifuged at 4 °C and 3000 rpm for 15 min, and the serum was stored at −80 °C.

Approximately 5×10^4 cells/mL HepG2 immortalized rat liver cells were grown under an atmosphere of 5% CO_2 at 37 °C in KRP buffer solution. Cells were cultured in 96-well plates (200 μL/hole). After 24 h, the cell monolayer was sufficient to achieve confluence. Then, culture medium was removed, followed by washing three times using KRP buffer solution. Next, 2-NBDG-KRP buffer solution (100 μmol/L) was added and incubated with the cells for 60 min, and the supernatants were discarded.

The FZYLD and blank sera were prepared. The FZYLD serum containing 5, 10, 15, 20, 25, and 30% was used to culture the 2-NBDG labeled cells for 12, 24, and 48 h. The proliferation inhibition rate and IC_{50} were detected using MTT assay. After adding 70 μL of phosphate buffer containing 1% Triton X-100 and avoiding light for 10 min, the intensities were measured using a fluorescence enzyme labeling instrument (excitation and emission wavelengths 465 and 540 nm). The morphology of HepG2 cell-labeled 2-NBDG was observed using a fluorescence inverted microscopy at 100× magnification.

Statistical Analysis

Data are expressed as the mean ± standard error of the mean. All statistical analyses were performed using the SPSS software. Statistical differences among multiple groups were analyzed by one-way analysis of variance followed by *t*-test. Statistical significance was set at $p < 0.05$.

Results

Effect of FZYLD on Blood Pressure and Heart Rate in a Rat Model of HCC

The mean SBP values (mmHg) in the model and low- and high-dose groups were 90.97 ± 7.82, 110.63 ± 11.20, and 125.11 ± 9.17, respectively, whereas DBP values were 78.45 ± 5.96, 85.72 ± 7.48, and 93.56 ± 6.81, respectively. The mean HR values in the model and low- and high-dose groups were 195.34 ± 38.69, 247.88 ± 46.07, and 296.39 ± 53.98, respectively (Table 2). With FZYLD medication, SBP, DBP, and HR levels continued to increase. Mice in the two FZYLD-treated groups showed significantly higher levels of all cardiac indicators than those in the HCC model group. All p-values were lower than 0.01, except that of DBP values measured for the low-dose group, which exhibited $p < 0.05$.

Breathing rate was recorded using the MedLab system for 30 min. In the model and low- and high-dose groups, the V mean values (mL/s) were 474.85 ± 23.75, 494.56 ± 22.22, and 541.78 ± 27.54 and Vt (mL) values were 7.55 ± 1.21, 9.46 ± 1.34, and 11.43 ± 2.98, respectively. The mean Ptp values (cm.H_2O) were 10.12 ± 2.13, 8.89 ± 1.78, and 8.41 ± 1.56, respectively (Table 2). FZYLD treatment resulted in a significant elevation in V, Vt, and Ptp compared with those of the HCC model group ($p < 0.01$ or $p < 0.05$) in the FZYLD group, with the results showing a better effect of the high dose than that of the low dose. Experimental results showed that FZYLD improved pulmonary function in HCC rats.

Immobility Time in the Tail Suspension Test

Before modeling, no significant difference was detected in the tail suspension test among all rats ($p > 0.05$). The immobility times in the tail suspension test in the model and low- and high-dose groups were 247.42 ± 9.04, 198.85 ± 10.74, and 177.01 ± 9.52, respectively, ($p < 0.01$). FZYLD decreased the immobility time of the rats in the tail suspension test in a dose-dependent manner (Table 2).

Table 2 Cardiopulmonary Function and Tail Suspension Test Results of Rats (n=7, $\bar{x} \pm sd$)

Groups	Blood Pressure and Heart Rate			Tidal Volume, Airway Flow and Trans Pulmonary Pressure			Immobility Time in Tail		
	SBP (mmHg)	DBP (mmHg)	HR (Beats per Minute)	V (mL/s)	Vt (mL)	Ptp (cm.H_2O)	Before Molding (s)	After Molding (s)	After Treating (s)
Normal control	130.02±6.61	97.23±3.15	298.28±22.47	550.65±16.43	13.12±1.54	8.05±0.99			
HCC model	90.97±7.82	78.45±5.96	195.34±38.69	474.85±23.75	7.55±1.21	10.12±2.13	137.48±7.67	247.42±9.04	
Low dose	110.63±11.20▲▲	85.72±7.48▲	247.88±46.07▲▲	494.56±22.22▲	9.46±2.34▲▲	8.89±1.78▲	139.36±10.11	249.23±10.18	198.85±10.74▲▲
High dose	125.11±9.17▲▲	93.56±6.81▲▲	296.39±53.98▲▲	541.78±27.54▲▲	11.43±2.98▲▲	8.41±1.56▲▲	141.07±7.54	245.56±10.73	177.01±9.52▲▲

Note: Remark:FZYLD vs model, ▲p<0.05, ▲▲p<0.01.

https://doi.org/10.2147/CMAR.S377621

FZYLD Tumor Inhibition Rate

Compared with those of the model group, reduced tumor weight and size were detected in the treatment groups ($p < 0.05$). The tumor inhibition ratios were 27.35 and 27.77%, respectively, for the low- and high-dose groups, without any significant difference in the tumor inhibition rate between the two doses ($p > 0.05$) (Figure 1).

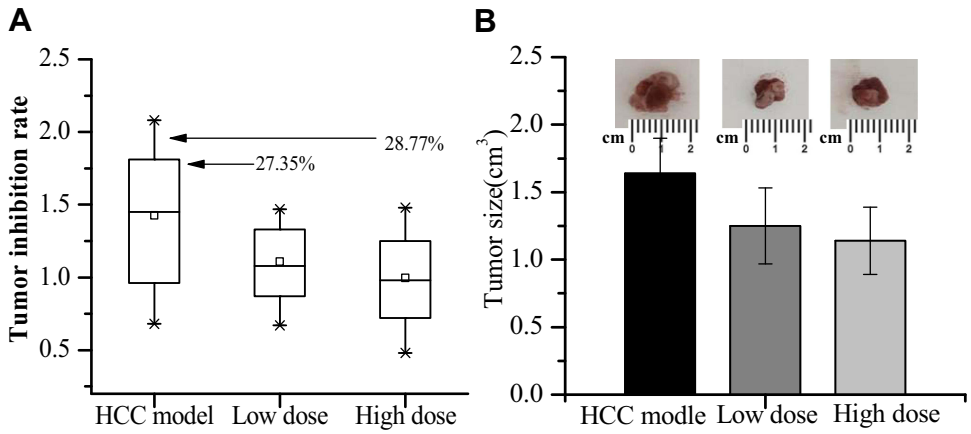

Figure 1 Comparison of the tumor inhibition rate. (**A**) Tumor inhibition rate; (**B**) Tumor size. Data are represented as mean ± *sd* (n=7).

Profiling of Endogenous Serum Metabolites Using NMR

Figure 2A and B shows a typical 1H-NMR spectrum of the serum of rats in the model group. The CPMG pulse sequence can suppress the signals of macromolecules such as lipids and obtain the metabolic information of small molecules such as glucose, amino acids, and Krebs cycle (TCA) intermediates (lactate). Figure 2C and D shows the 1H-NMR spectrum of the LED pulse sequence, which can block the signal of small molecules, such as amino acids, and obtain the reliability of changes in macromolecules metabolites, such as lipids. These metabolites contained O-acetyl glycoprotein, N-acetyl glycoprotein, and fatty acids.

SIMCA-P software (v10.04, Umetrics, Umeå, Sweden) was used for multivariate statistical analysis. The data were pretreated with average central (mean centering) or Pareto scale (Pareto scaling) and then analyzed by PCA. To strengthen the difference between groups, PLS-DA or OSC analysis was used. The results are expressed in the form of score chart (scores plot) and load chart (loading plot). The chemical shifts of representative metabolites in the serum are shown in Tables 3 and 4. The PCA analysis results are shown in Figure 3A and B and Figure 4A and B, and PLS-DA analysis results are shown in Figure 3C and D and Figure 4C and D.

PCA and PLS-DA, based on the profiling of NMR CPMG spectra of serum samples from the HCC model group and the two FZYLD groups, were employed to explore the intrinsic metabolic differences between these rats. Samples from different groups were classified, and the results were presented in the form of a score plot, where each mark represents an individual sample (to reveal the group clusters), and a loading plot, where each coordinate represents one 1H-NMR spectral region, to identify the classification variables. The PCA and PLS-DA score plots both show a division of HCC and FZYLD groups into two distinct clusters, clearly separated based on the first PCA component. However, the low- and high-dose groups are not separated based on the second PCA component, indicating that both FZYLD groups are consistent.

Seven metabolites were identified. Compared to those of the FZYLD group, the HCC model group showed higher levels of endogenous serum metabolites, valine (Val), 3-hydroxybutyrate, and lactate (Lac), which were markedly decreased after the rats received FZYLD. Lower levels of lipoprotein, alanine (Ala), and glucose were found in the serum of the rats of the HCC group compared with those of both FZYLD groups. However, they were markedly increased after the rats received FZYLD (Table 3).

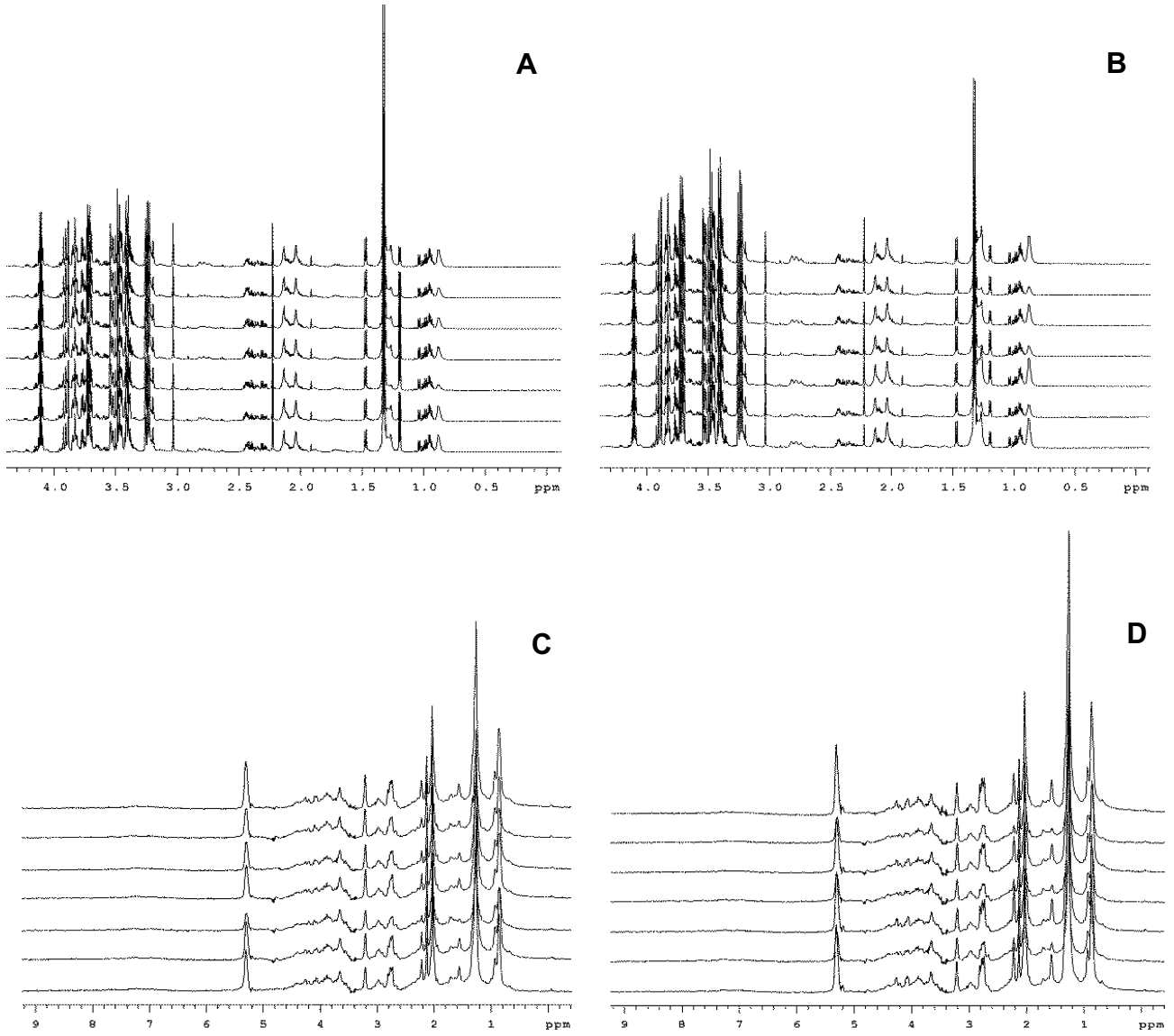

Figure 2 1H-NMR spectrum of the serum (n=7). **(A)** Model group rats by CPMG pulse sequence; (**B**) Low doges group by CPMG pulse sequence; **(C)** Model group rats by LED pulse sequence; (**D**) Low doges group by LED pulse sequence.

Table 3 1H-NMR CPMG Data and Assignments of the Metabolites in Rat Serum

Chemical Shift (ppm)	Compound	HCC Model Group	Low Dose Group	High Dose Group	Concentration Change After Treating
0.86, 0.90	Lipoprotein	134.52/97.67	185.22/128.21	184.99/128.15	↑
0.98, 1.02	Val	124.91/64.84	103.13/54.31	81.035/39.96	↓
1.18	3-hydroxybutyrate	169.94	98.99	45.68	↓
1.26, 1.30	Lipoprotein	753.24/172.59	771.54/267.59	782.73/252.76	↑
1.34, 4.10	Lac	899.58/324.83	836.69/300.21	835.41/293.86	↓
1.46	Ala	159.66	158.89	161.81	—
3.40–4.00	Sugars	486.57	556.68	571.49	↑

Note: The symbols indicate: ↑ (Rise), ↓ (Fall), — (No difference).

PCA and PLS-DA, based on the profiling of NMR LED spectra of the serum samples from the HCC model group and both FZYLD groups, were employed to explore the intrinsic metabolic differences between these rats. Samples from different groups were classified, and the results were presented in the form of a score plot, where each mark represents an

Table 4 1H-NMR LED Data and Assignments of the Metabolites in Rat Serum

Chemical Shift (ppm)	Compound	HCC Model Group	Low Dose Group	High Dose Group	Concentration Change After Treating
0.86, 0.82	**HDL**	474.49/195.54	486.56/232.98	485.39/202.12	↑
1.26	**VLDL**	793.62	976.18	810.06	↑
1.34,1.3	**LDL**	210.32/491.51	246.90/614.61	236.45/545.54	↑
1.58	**Lipid**	108.82	121.76	121.98	↑
2.02	**NAc**	466.44	464.07	490.48	↑
2.14	**OAc**	239.11	244.83	265.47	↑
2.22	**FA**	132.33	161.94	143.06	↑
3.22	**PtdCho**	127.26	130.47	123.20	—
5.3, 5.26	**UFA**	238.47/105.47	235.89/104.28	214.26/86.35	↓

Note: The symbols indicate: ↑ (Rise), ↓ (Fall), — (No difference).

individual sample (to reveal the group clusters), and a loading plot, where each coordinate represents one 1H-NMR spectral region, to identify the classification variables. As displayed in Figures 3 and 4, the PCA and PLS-DA score plots show a division of the HCC and FZYLD groups into two distinct clusters clearly separated based on PCA component 1. However, the low- and high-dose groups are not separated based on PCA component 2, indicating that both FZYLD groups are consistent.

Nine metabolites were identified. Compared to those of the FZYLD group, the HCC model group showed lower levels of endogenous serum metabolites, very low-density lipoprotein (VLDL), low-density lipoprotein (LDL), high-

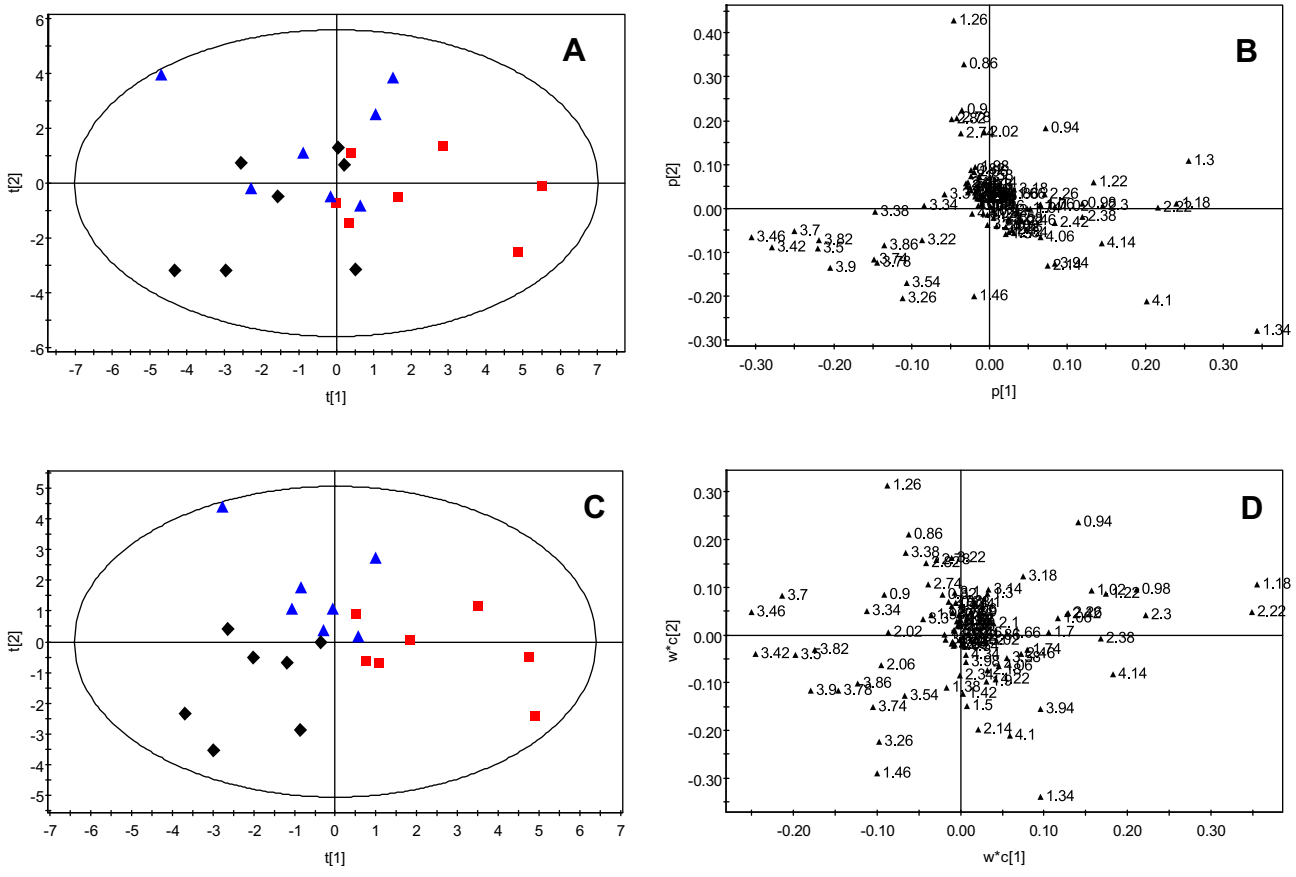

Figure 3 PCA scores plots and loading (p[1] p[2]) plots of ^{1}H NMR CPMG spectra and PLS-DA scores plots and loading (w*c[1] w*c[2]) plots of ^{1}H NMR CPMG spectra. (**A**) PCA scores plot between FZYLD groups and model group; (**B**) Intrinsic metabolic differences between FZYLD groups and model group; R2X(cum)=61.7%; Q2(cum) =38.3%. (**C**) PLS-DA scores plot between FZYLD groups and model group; (**D**) Intrinsic metabolic differences between FZYLD groups and model group. R2X(cum)=57.5% R2Y(cum)=56.2%; Q2(cum)=37.3%. Model group (■), Low dose group (▲), High dose group (◆).

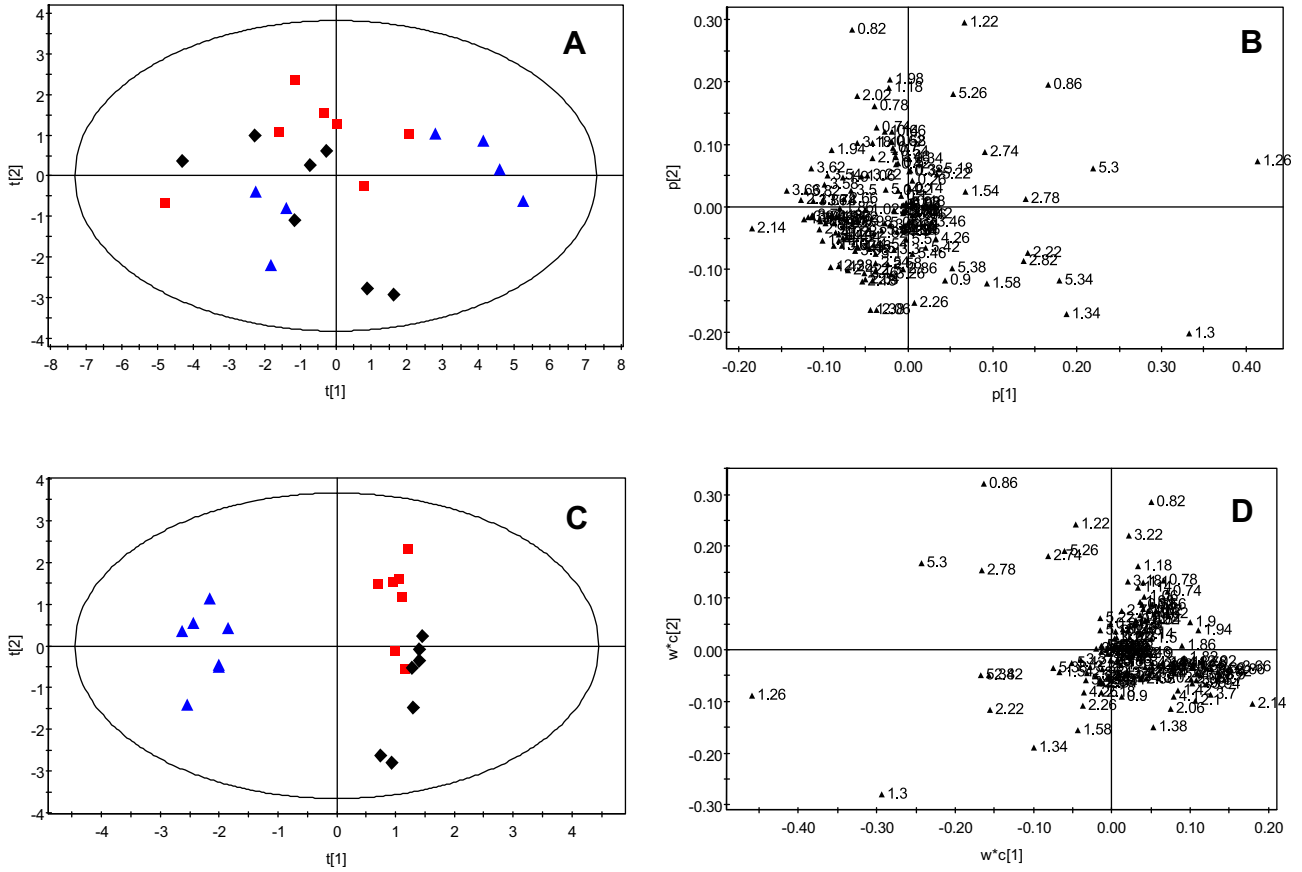

Figure 4 PCA scores plots and loading (p[1] p[2]) plots of ^{1}H NMR LED spectra and PLS-DA scores plots and loading (w*c[1] w*c[2]) plots of ^{1}H NMR LED spectra. (**A**) PCA scores plot between FZYLD groups and model group; (**B**) Intrinsic metabolic differences between FZYLD groups and model group; R2X(cum)=78.9%; Q2(cum)= 72.1%.(**C**) PCA scores plot between FZYLD groups and model group; (**D**) Intrinsic metabolic differences between FZYLD groups and model group; R2X(cum)=61.5%; R2Y (cum)=22.9%; Q2(cum)= 63.5%. Model group (■), Low dose group (▲), High dose group (◆).

density lipoprotein (HDL), fatty acid (FA), N-acetyl glycoprotein (NAc), and O-acetyl glycoprotein (OAc). However, they were markedly increased after the rats received FZYLD. Higher levels of unsaturated fatty acid (UFA) were found in the serum of the rats of the HCC group compared with those of both FZYLD groups; however, UFA level markedly decreased after the rats received treatment. The content of lipid and phosphatidylcholine (PtdCho) was approximately the same before and after treatment. Lipid metabolism was better regulated using low-dose FZYLD than using high-dose FZYLD (Table 4).

Exogenous Metabolic Serum Profiling by LC-MS/MS

The HPLC fingerprints of rat serum were determined at different times. FZYLD was quickly absorbed and removed, and the drug concentration reached a maximum in 40 min; rats could metabolize various FZYLD ingredients in 300 min. Under experimental HPLC conditions, the rat serum fingerprints identified seven exogenous substances in the blood of FZYLD treated animals (labeled as 1–7). Peaks 1, 2, 3, and 7 were the major constituents (Figure 5).

The mass spectra revealed fragment patterns of seven compounds, and the chemical structure of the components was characterized based on the previous literature. The compounds were diosgenin, apigenin-7-O-acetyl-β-D-glucoside, calycosin-7-glucoside, ganoderic acid A, calycosin, formononetin, and methylnissolin (Table 5).

Effect of FZYLD-Containing Serum on HepG2 Cell Proliferation

The concentration of the drug-containing serum should be <30% the medium volume. Cellular viability was negatively correlated with the dose of the serum-containing FZYLD. HepG2 cells were labeled using 2-NBDG. Changes in cell proliferation at different time points were observed by co-culturing with different concentrations of FZYLD-containing

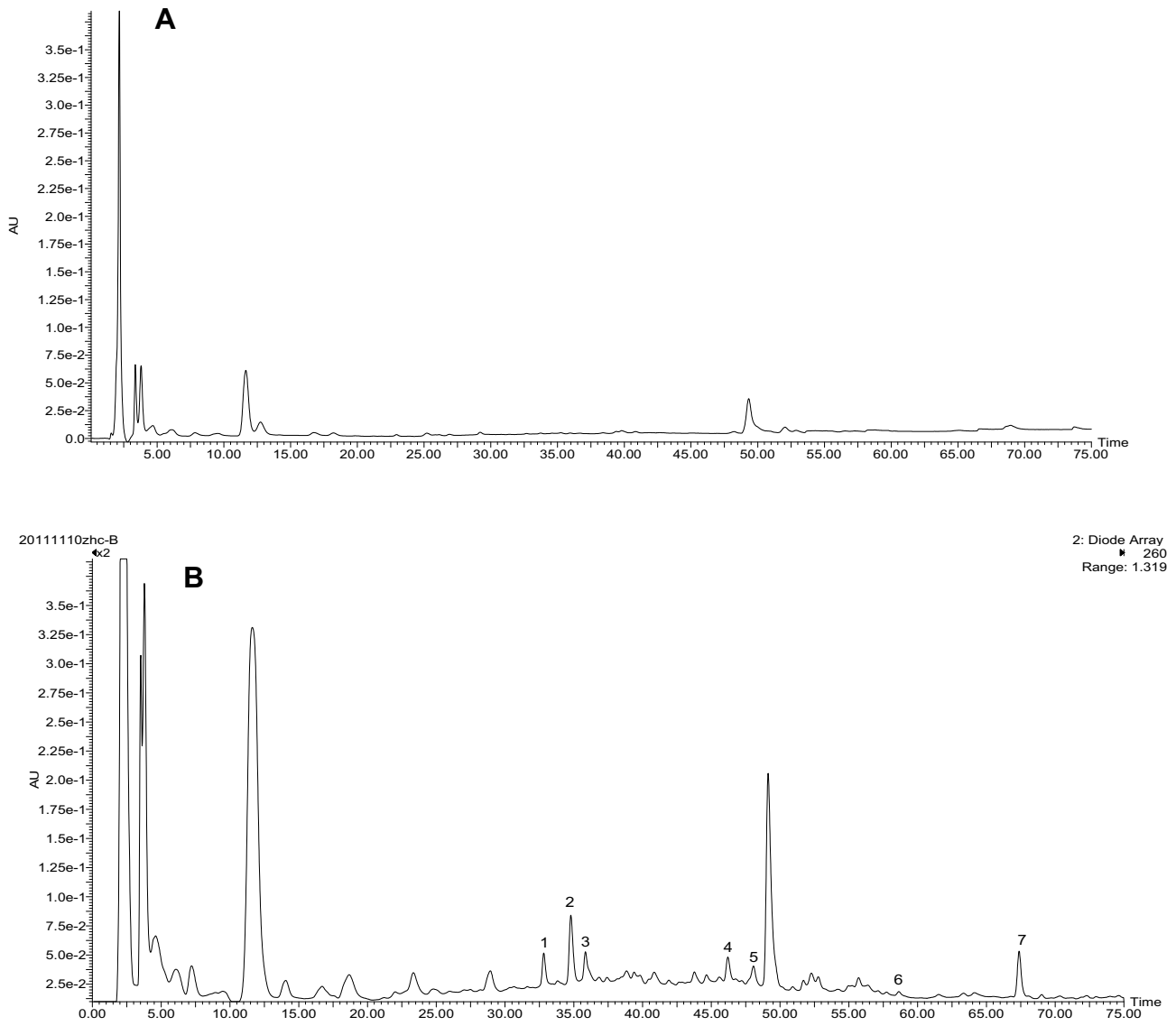

Figure 5 HPLC Chromatograms of rat blank and medicated serum. (**A**) Blank serum; (**B**) Medicated serum.

serum with the aid of fluorescent microscopy and an enzymatic marker. Incubation with drug serum at 5–30% concentrations for 12 or 24 h showed an increase in inhibition of HepG2 cells proliferation from 13.84 to 15.22% and from 10.97 to 31.39%, respectively, in a dose-dependent manner. HepG2 cells were incubated with serum-containing

Table 5 Identification of 7 Constituents Immigrating to Serum After Rat Oral FZYLD

Peak No.	ESI -MS		Deduce Compound	Structure
	m/z (+)	m/z (-)		
1	$[M+H]^+$ 415 $[M+Na]^+$437		Diosgenin	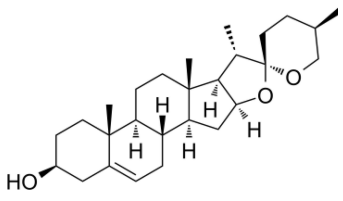

(*Continued*)

Table 5 (Continued).

Peak No.	ESI -MS		Deduce Compound	Structure
	m/z (+)	m/z (-)		
2	$[M+H]^+$ 475		Apigenin-7-O- acetyl-β-D-glucoside	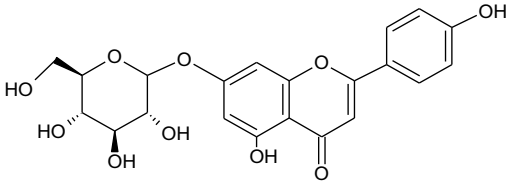
3	$[M+H]^+$447 $[M+H-162]^+$ 285	$[M-H]^-$283	Calycosin-7-glucoside	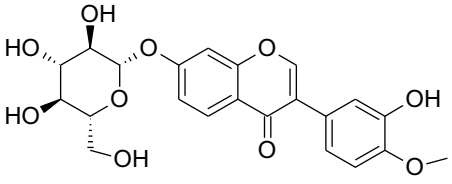
4	$[M+H]^+$ 516	[M]515	Ganoderic acid A	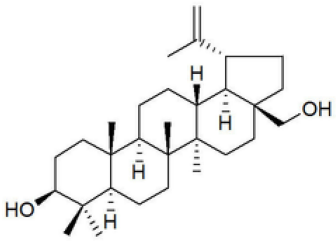
5	$[M+H]^+$285	$[M-H]^-$283	Calycosin	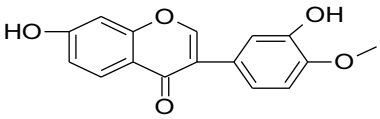
6	$[M+H]^+$269 $[M+Na]^+$291	$[M-H]^-$267	Formononetin	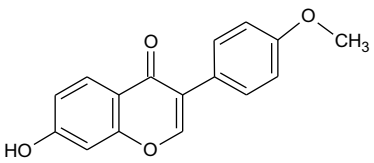
7	$[M+H]^+$ 301		Methylnissolin	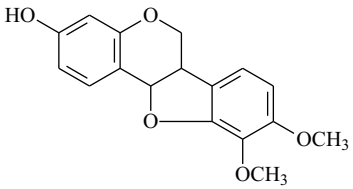

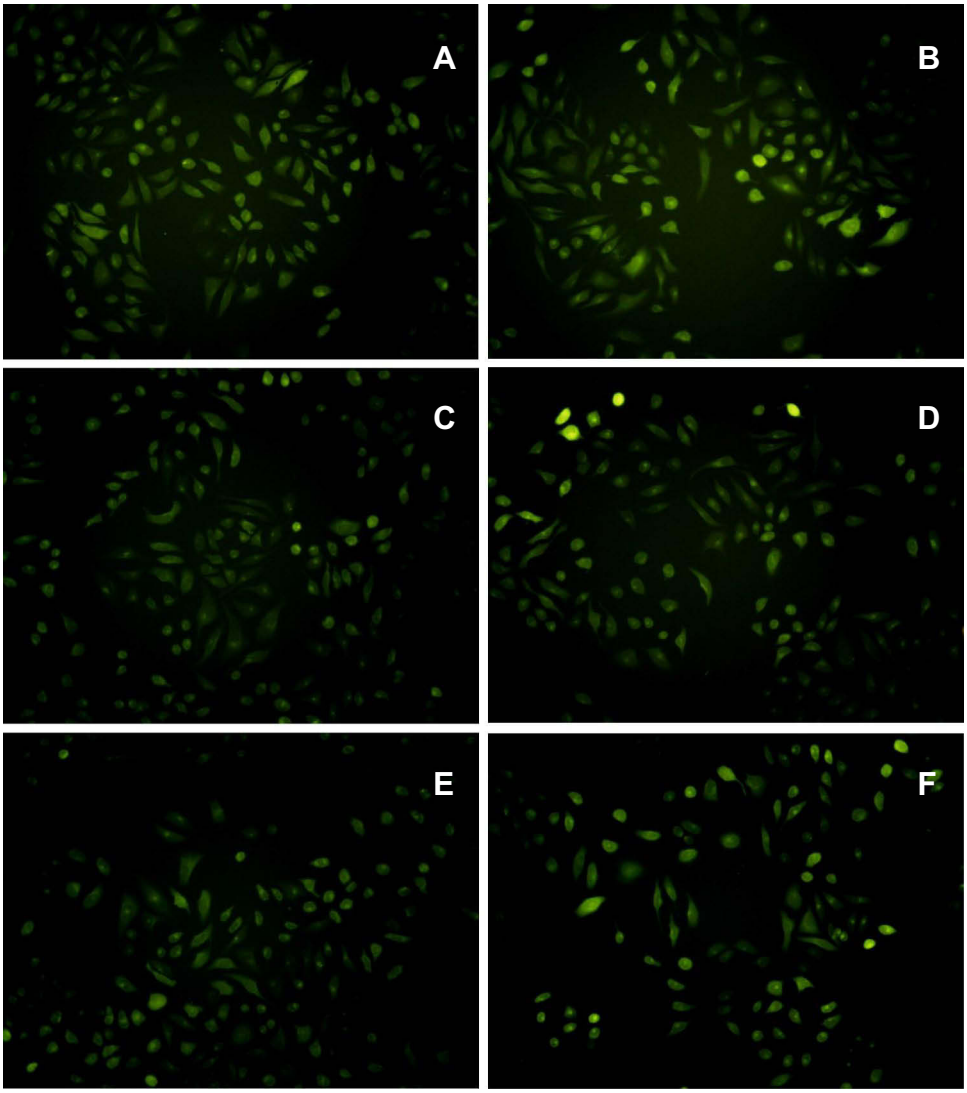

Figure 6 Fluorescence micrographs of 2-NBDG labeled HepG2 cells incubated using serum contained FZYLD for 48 h. (**A**) 2-NBDG labeled HepG2 cells (negative control); (**B**) 5% drug serum inhibits the proliferation of HepG2 cell; (**C**) 10% drug serum inhibits the proliferation of HepG2 cell; (**D**) 15% drug serum inhibits the proliferation of HepG2 cell; (**E**) 20% drug serum inhibits the proliferation of HepG2 cell; (**F**) 25% drug serum inhibits the proliferation of HepG2 cell; (n = 5).

FZYLD for 48 h compared to a negative control. The inhibition rate was 13.84% ± 3.43%, 14.85% ± 3.02%, 18.10% ± 4.57%, 33.22% ± 4.38%, 52.68% ±4.65%, and 65.66% ± 4.84%, respectively. IC_{50} was found to be 24.31%. FZYLD-containing serum inhibited HepG2 cell proliferation and promoted apoptosis. The detailed data are available in Figure 6.

Discussion

FZYLD, a multi-herb formula, is our hospital prescription. It has been used for more than 10 years to cure liver tumors and can improve clinical symptoms, decelerate weakening after chemotherapy or radiation, improve the quality of life, and prolong the survival time of patients with tumors. However, the mechanism underlying these effects is still unclear.

In the terminal stage of cancer, multiple organ failure leads to weakness that may be accompanied with cardiopulmonary function decline. The decline of the physical health of HCC model group is associated with impaired heart function, hypotension, bradycardia, decreased cardiac output, and reduced pulmonary function parameters, V and Vt but increased Ptp. Treatment of HCC rats with FZYLD showed apparent changes in cardiopulmonary function indices.

To evaluate the effect of FZYLD on serum endogenous metabolism in HCC rats, we used metabolomics and found that PCA and PLS-DA analyses of serum NMR spectrum and the metabolic spectrum in both HCC and FZYLD groups were substantially different. Because tumor cells consume a lot of energy to sustain their proliferation, serum levels of glucose, lipoprotein, HDL, lipids, NAc, acetate, VLDL, LDL, and FA were decreased, whereas the contents of Lac, Val, 3-hydroxybutyrate, and UFA were increased. A high concentration of lactic acid is a marker of tumor metabolic adaptability. The production and accumulation of lactic acid in vivo can promote tumor growth and metastasis and is related to poor tumor prognosis. Furthermore, tumor cell growth requires a large amount of valine, and valine restriction can prevent the synthesis of tumor cell structural proteins and enzyme proteins, thereby obstructing energy metabolism. After two weeks of FZYLD treatment, some indicators such as lipoprotein, glucose, HDL, LDL, valine, and lactic acid levels were recovered to some extent. FZYLD reverted the metabolic and energy disorders in HCC rats.

FZYLD-containing serum inhibited the proliferation of HepG2 cells. HPLC/MS/MS was used to determine exogenous metabolites in serum. Diosgenin, apigenin-7-O-acetyl-β-D-glucoside, calycosin-7-glucoside, ganoderic acid A, calycosin, formononetin, and methylnissolin were detected. The fragment ion peak m/z 285 of calycosin may be a metabolite produced by deglycosylation to remove a glucoside from calycosin-7-glucoside. In addition, calycosin and formononetin are original constituents of *Radix astragali* in FZYLD and potential metabolites of campanulin and ononin that lose a glucoside by glucuronic acid reaction.

Dioscoreae rhizoma contains a large amount of diosgenin. A reduction in HepG2 cell viability was observed due to diosgenin treatment at concentrations >30 μmol/L, which could be attributed to genetic instability, cell cycle disruption, and cell death.[22] Apigenin-7-O-acetyl-β-D-glucoside derived from Fructus ligustri lucid reduced HepG2 cell viability and induced apoptotic cell death. Apigenin induced a dose-related elevation of intracellular reactive oxygen species levels, whereas NADPH oxidase activation plays an essential role in apoptosis induced by apigenin in HepG2 cells. These results further suggest that apigenin may be valuable for the therapeutic management of human hepatomas.[23] Ganoderic acid A promoted cisplatin-induced cell death by enhancing the sensitivity of HepG2 cells to cisplatin mainly via suppression of the signal transducer and activator of transcription 3, suggesting a potential therapeutic effect of ganoderic acid A in combination with chemotherapeutic agents for cancer treatment.[24] Calycosin-7-glucoside, calycosin, formononetin, and methylnissolin are derived from *Radix astragali*. Calycosin is the hydrolysed material of calycosin-7-glucoside. It inhibits proliferation and promotes apoptosis of a variety of cancer cell types, such as HepG2, HCT116, and MCF-7,[25] whereas formononetin showed a mild cytotoxic effect on HepG2 cells with an IC_{50} of 200 μmol/L, which implies a remarkable anti-tumor activity in human hepatoma cells.[26]

Conclusion

The findings of this study indicate that FZYLD ameliorated metabolite changes in the serum of a rat model of HCC. This effect is mainly related to immune function, energy, and lipid metabolism. Seven bioactive components of FZYLD were detected in the blood. This study will help to better understand the underlying mechanisms of FZYLD in attenuating fatigue and low immunity. The combined method developed herein offers an efficient way for the clinical application of bioactive natural compounds and understanding the mechanisms of traditional Chinese medicine.

Ethics Approval and Informed Consent

Animal experiments were carried out in accordance with the Guidelines for Institutional Animal Ethics and were approved by the Committee of the Second Affiliated Hospital of Fujian University of Traditional Chinese Medicine (License number: FJTCM-IAEC2011001).

Author Contributions

All authors made a significant contribution to the work reported, whether that is in the conception, study design, execution, acquisition of data, analysis and interpretation, or in all these areas; took part in drafting, revising or critically reviewing the article; gave final approval of the version to be published; have agreed on the journal to which the article has been submitted; and agree to be accountable for all aspects of the work.

Funding

The authors give thanks to Project 82174462, supported by the National Natural Science Foundation of China and Fujian Natural Science Foundation (2020J01249); supported by Central Committee to Guide Local Science and Technology Development (Grants No. 2020L3012), the authors acknowledge Bethune Medical Science Research Foundation Project (B19003CS), and the Professional technical service platform of research & development of traditional Chinese medicine & health products (14C26243501795).

Disclosure

The authors declared that the research was conducted in the absence of any commercial or financial relationships that could be construed as a potential conflict of interest.

References

1. Xu J, Yang Y. Traditional Chinese medicine in the Chinese health care system. *Health Policy*. 2009;90(2–3):133–139. doi:10.1016/j.healthpol.2008.09.003
2. Shibata MA, Khan IA, Iinuma MK, et al. Natural products for medicine. *J Biomed Biotechnol*. 2012;2012:1–7. doi:10.1155/2012/147120
3. Pang WS, Lin SD, Dai QW, Zhang HC, Hu J. Antitussive activity of Pseudostellaria heterophylla (Miq.) Pax extracts and improve in lung function on the multicytokines adjusting. *Molecules*. 2011;16(4):3360–3370. doi:10.3390/molecules16043360
4. Su BL, Kan YJ, Xie JW, Hu J, Pang WS. Relevance of the pharmacokinetic and pharmacodynamic profiles of Puerariae lobatae radix to aggregation of multi-component molecules in aqueous decoctions. *Molecules*. 2016;21(7):845. doi:10.3390/molecules21070845
5. Chen JL, Pang WS, Shi WT, et al. Structural elucidation of a novel polysaccharide from Pseudostellaria heterophylla and stimulating glucose uptake in cells and distributing in rats by oral. *Molecules*. 2016;21(9):1233. doi:10.3390/molecules21091233
6. Pharmacopoeia Commission. *Pharmacopoeia of the People's Republic of China*. Beijing, China: Medical Science and Technology Press; Vol. 1, 2015:15–380.
7. Chen LW, Lin J, Chen W, Zhang WP. Effect of Chinese herbal medicine on patients with primary hepatic carcinoma in III stage during perioperational period: a report of 42 cases. *Chin J Integr Tradit West Med*. 2005;25:832–834.
8. Zhao HJ, Du J, Chen X, et al. Clinical study of Fuzheng Yiliu recipe combined with microwave ablation on hepatocellular carcinoma. *Chin J Integr Tradit West Med*. 2013;32:32–34.
9. Chen LW, Du J, Tan JW, Huang ZW. Clinical study of Chinese herbs combined with operation on the primary hepatocarcinoma. *J Fujian Coll TCM*. 2005;15:6–8.
10. Cao ZY, Du J. Effects of Fuzheng Yiliu decoction on apoptosis related factors expression of H22 tumor-bearing ICR mice. *J Fujian Univ TCM*. 2013;22:25–28.
11. Hu HX, Cao ZY, Liu ZZ, Chen X, Du J. Effects of Fuzheng Yiliu decoction on expressions of a proliferation-inducing ligand and its receptors in hepatocellular carcinoma tissues. *J Fujian Univ TCM*. 2011;21:27–29.
12. Zhang YQ, Chen XZ, Cao ZY, Du J. Intervention effect of Fuzheng Yiliu decoction on proliferation and apoptosis of hepatoma HepG2 cells. *J Fujian Univ TCM*. 2010;20:30–33.
13. Cao ZY, Du J, Chen LW, Liao LM, Zheng LP, Lin W. Influence of Chinese compound prescription on humoral immune in mice with hepatic carcinoma transplanted subcutaneously. *J Fujian Coll TCM*. 2007;17:33–34.
14. Chen LW, Du J, Dai QW, Zhang HC, Pang WS, Hu J. Prediction of anti-tumor chemical probes of a traditional Chinese medicine formula by HPLC fingerprinting combined with molecular docking. *Eur J Med Chem*. 2014;83:294–306. doi:10.1016/j.ejmech.2014.06.037
15. Zheng CS, Chen LW, Du J, Ye HZ. Study on anti-tumor mechanism of Chinese medicine Fuzhengyiliufufang by molecular docking method. *Chin J Clin Pharmacol Ther*. 2007;12:892–895.
16. Zheng XF, Tian JS, Liu P, Xing J, Qin XM. Analysis of the restorative effect of Bu-zhong-yi-qi-tang in thespleen-qi deficiency ratmodelusing 1H-NMR-based metabonomics. *J Ethnopharmacol*. 2014;151(2):912–920. doi:10.1016/j.jep.2013.12.001
17. Wang Y, Li ZF, Chen JX, et al. Study of mini-pig serum of coronary heart disease (Chronic Myocardial I Schemia) with syndrome of blood stasis based on nuclear magnetic resonance metabolomics. *Chin J Anal Chem*. 2011;39:1274–1278.
18. Shan JJ, Qian WJ, Peng LX, et al. A comparative pharmacokinetic study by UHPLC-MS/MS of main active compounds after oral administration of zushima-gancao extract in normal and adjuvant-induced arthritis rats. *Molecules*. 2018;23(1):227. doi:10.3390/molecules23010227
19. Pang WS, Yang HW, Wu ZS, Huang MX, Hu J. LC-MS/MS in MRM mode for detection and structural identification of synthetic hypoglycemic drugs added illegally to 'Natural' anti-diabetic herbal products. *Chromatographia*. 2009;70(9–10):1353–1359. doi:10.1365/s10337-009-1344-0
20. Peres RG, Tonin FG, Tavares MFM, Rodriguez-Amaya DB. HPLC-DAD-ESI/MS identification and quantification of phenolic compounds in Ilex paraguariensis beverages and on-line evaluation of individual antioxidant activity. *Molecules*. 2013;18(4):3859–3871. doi:10.3390/molecules18043859
21. Xu C, Yang Y, Yi SH, Li X, Zhang Q, Chen Gui H. Standardization of rat stable orthotopic liver transplantation model and comparison of the effect of two liver graft perfusion methods. *Nan Fang Yi Ke Da Xue Xue Bao*. 2006;26(11):1556–1558.
22. Cruz MS, Navoni JA, da Costa Xavier LA, et al. Diosgenin induces genotoxic and mutagenic effects on HepG2 cells. *Food Chem Toxicol*. 2018;120:98–103. doi:10.1016/j.fct.2018.07.011
23. Choi SI, Jeong CS, Cho SY, Yee YS. Mechanism of apoptosis induced by apigenin in hepG2 human hepatoma cells: involvement of reactive oxygen species generated by NADPH oxidase. *Arch Pharm Res*. 2007;30(10):1328–1335. doi:10.1007/BF02980274
24. Yao XY, Li GL, Xu H, Lü CT. Inhibition of the JAK-STAT3 signaling pathway by ganoderic acid A enhances chemosensitivity of HepG2 cells to cisplatin. *Planta Med*. 2012;78(16):1740–1748. doi:10.1055/s-0032-1315303
25. Fu XW, Wang X, Pu WC, XR Li, Wang C. Synthesis and antitumor activities of calycosin and its derivatives. *Chin J Synth Chem*. 2015;23(3):223–226.
26. Cao ZJ, Cai XY, Fang W, Chen HS, Zhang HN, Zhang YL. Chemical compositions of Cortex Juglans Mandshurica and their activity screening of anti-hepatocarcinoma effect. *Shandong Med J*. 2014;54(29):1–3.